JOURNAL OF AGRICULTURAL AND FOOD CHEMISTRY

J. Agric. Food Chem. **2008,** *56,* 8609–8618 **8609**

Molecular Structures of Gellan Gum Imaged with Atomic Force Microscopy in Relation to the Rheological Behavior in Aqueous Systems in the Presence or Absence of Various Cations

TAKAHIRO FUNAMI,*,† SAKIE NODA,† MAKOTO NAKAUMA,† SAYAKA ISHIHARA,† RHEO TAKAHASHI,‡ SAPHWAN AL-ASSAF,§ SHINYA IKEDA,|| KATSUYOSHI NISHINARI,§,|| AND GLYN O. PHILLIPS§,⊥

Hydrocolloid Laboratory, San-Ei Gen F.F.I., Inc., 1-1-11 Sanwa-cho, Toyonaka, Osaka 561-8588, Japan; Department of Chemistry and Chemical Biology, Graduate School of Engineering, Gunma University, 1-5-1 Tenjin-cho, Kiryu, Gunma 376-8515, Japan; Glyn O. Phillips Hydrocolloid Research Centre, North East Wales Institute, Plas Coch, Mold Road, Wrexham LL11 2AW, United Kingdom; Department of Food and Human Health Sciences, Graduate School of Human Life Science, Osaka City University, 3-3-138 Sugimoto, Sumiyoshi-ku, Osaka 558-8585, Japan; and Phillips Hydrocolloids Research Ltd., 45 Old Bond Street, London W1S 4AQ, United Kingdom

Aqueous solutions of gellan gum with comparable molecular masses but with different acyl contents were investigated by atomic force microscopy and rheological measurements in the presence or absence of various cations. For a high-acyl sample, no continuous network structures were identified microscopically, except in the presence of Ca^{2+}, where structural inhomogeneity was the highest in terms of the height distribution of molecular assemblies. Rheological thermal hysteresis between sol−gel transitions was detected in the presence of K^+ and Ca^{2+}, particularly Ca^{2+}. The storage modulus at 20 °C was larger in the order $Na^+ < Ca^{2+} < K^+$. For a low-acyl sample, continuous network structures were identified in the presence of each cation, involving greater thermal hysteresis than the corresponding data for the high-acyl sample. Structural homogeneity was the highest in the presence of K^+. Thermal hysteresis and elasticity of the system were discussed in terms of continuousness and homogeneity of network structures.

KEYWORDS: Gellan gum; supermolecular structures; atomic force microscopy; rheology; cations

INTRODUCTION

Gellan gum is a linear, anionic heteropolysaccharide produced by a microorganism, *Sphingomonas elodea* (*1, 2*) and has been used in the food industry mainly as a gelling agent. Gellan gum has a molecular structure based on a tetrasaccharide repeating unit composed of (1−3)-β-D-glucose, (1−4)-β-D-glucuronic acid, (1−4)-β-D-glucose, and (1−4)-α-L-rhamnose as the backbone with acyl substituents of L-glycerate and acetate at the C-2 and C-6 (approximately 50%) positions of the (1−3)-linked D-glucose, respectively (*3*). Gellan gum forms gels with various physical and textural attributes depending on the acyl content and also on the types and concentrations of cations added. Generally, the low-acyl type forms texturally hard and brittle gels in the presence of cations, particularly gel-promoting cations, including Ca^{2+} and K^+, with increased thermoirreversibility, whereas the high-acyl type forms texturally soft and elastic gels even in the absence of cations (*4, 5*).

The gelation mechanism of gellan gum has been investigated in aqueous systems (*6*−*9*). The gelation process is generally considered to involve two separate thermoreversible steps. Molecules of gellan gum are in a disordered coil (single chain) upon heating in aqueous solutions. The molecules transform into an ordered double helical conformation upon subsequent cooling, followed by associations between the helices, which results in the formation of thermoreversible weak gels. One gelation mechanism (*7, 10, 11*) proposes the formation of distinct junction zones, with disordered flexible polymer chains connecting adjacent junction zones. In this model, the elasticity would arise from the entropic contributions of these flexible polymer chains. Another mechanism has been proposed based on light scattering measurements (*12*) and atomic force microscopy (AFM) studies (*11, 13, 14*) without assuming the presence of distinct junction zones and disordered flexible polymer chains. This is denominated as the "fibrous model", where macroscopic

* To whom correspondence should be addressed. Phone: +81-6-6333-0521. Fax: +81-6-6333-2076. E-mail: tfunami@saneigenffi.co.jp.
† San-Ei Gen F.F.I., Inc.
‡ Gunma University.
§ Glyn O. Philips Hydrocolloid Research Centre.
|| Osaka City University.
⊥ Phillips Hydrocolloids Research Ltd.

10.1021/jf8007713 CCC: $40.75
Published on Web 08/19/2008

network structures develop through the formation of nonassociated fibers or strands via either elongation or branching, percolating throughout the entity. In this model, the elasticity would arise mainly in an enthalpic manner from stretching and bending of these fibrous strands.

The effects of cations on the gelation of gellan gum have been investigated (*4, 5, 14*−*19*) because the carboxyl side groups within the backbone can be affected greatly by inherent counterions and cations added. The main function of cations is to shield electrostatic repulsion between the helices and thus to promote interhelical associations via hydrogen bonds. However, the effectiveness varies between divalent cations and monovalent cations and even within monovalent cations. Divalent cations such as Ca^{2+} and Mg^{2+} fortify the gel matrixes efficiently at lower concentrations than monovalent cations (*4, 5, 15*), and this is attributed to the formation of direct polyanion−cation−polyanion linkages (*20*) between adjacent double helices. The binding force of the polyanion−cation−polyanion linkages would be stronger than that of the polyanion−cation−water−cation−polyanion linkages (*21*) formed in the presence of monovalent cations (*22*). Among monovalent cations, Li^+ and Na^+ are less effective in promoting gelation than K^+, Rb^+, and Cs^+ (*14, 16*−*18, 23*). Rheologically, the sol-to-gel and gel-to-sol transitions shift to higher temperatures upon the addition of cations, depending on the cationic species (*18, 24*−*26*) and also on the polymer concentration (*27, 28*). Immersion in salt solutions increases the gel elasticity of gellan gum, and this effect of salts is in the order $Li^+ < Na^+ < K^+ < Cs^+$ when compared at the same molar concentration (*29*). Bulky cations (e.g., tetramethylammonium) are known to prevent interhelical associations due to steric hindrance (*11, 13, 26*). In most studies so far, the deacylated type has been a target for investigations, and there is still insufficient information on the gelation behavior of the acylated type.

In the present study, well-characterized samples with comparable average molar masses but different acyl contents were investigated in terms of rheological and related microscopic properties to clarify the effect of cations on the gelation of gellan gum. Cations included Na^+ and K^+ as monovalent cations and Ca^{2+} as a divalent cation, all of which were used in the form of chloride salts. Our goal is to understand the gelation mechanism and the structure−function relationship of gellan gum, providing strategies for the best usage in the food industry.

MATERIALS AND METHODS

Materials. Two samples of gellan gum with different acyl contents were supplied by CP Kelco (San Diego, CA). These samples were denominated as HAGG (high-acyl gellan gum) and LAGG (low-acyl gellan gum). LAGG was prepared by a deacylation process under a certain alkaline condition using HAGG as the starting material. Both samples were purified by ethanol precipitation and subsequently changed to the sodium type as reported previously (*30*). NaCl, KCl, and $CaCl_2$ (Wako Pure Chemicals, Osaka, Japan) were all of reagent grade and used without further purification.

Methods. *Characterizations of Gellan Gum Samples.* The cation content (Na^+, K^+, and Ca^{2+}) was determined by elemental analysis using inductively coupled plasma optical emission spectrometry (ICP-OES) as reported previously (*30*). Acyl groups, including glycerate and acetate, were determined by high-performance ion chromatography (HPIC) based on the method of the gellan gum manufacturer. The weight-average molar mass (M_w) was determined by size exclusion chromatography coupled with multiangle laser light scattering (SEC−MALS) photometry using cadoxen (including cadomium oxide, ethylenediamine, and deionized water) as a solvent (*31*). The SEC system consisted of an LC-10AD$_{VP}$ HPLC pump (Shimadzu, Kyoto, Japan), an LC-10AC$_{VP}$ column oven (Shimadzu), and a TSKgel GMPW$_{XL}$ separation column (Tosoh Co., Tokyo, Japan). The solvent was circulated throughout the system at a flow rate of 0.25 mL/min. The MALS detections were carried out at 25 °C using a DAWN-EOS instrument (Wyatt Technology Co., Santa Barbara, CA) with a vertically polarized Ga−As laser at a wavelength of 684 nm. The scattering intensity was determined at angles from 22° to 157° simultaneously with multiple detectors. A 100 μL volume of gellan gum in aqueous solutions (1 mg/mL), prepared by dissolving the respective sample in cadoxen at room temperature with gentle stirring overnight, was injected into the SEC system after passing through PTFE filters of 0.45 μm pore size (ADVANTEC Toyo, Ltd., Tokyo, Japan). The increase in the refractive index with concentration (dn/dc, mL/g), determined using an OPTILAB DSP instrument (Wyatt Technology), was 0.139 mL/g.

Table 1. Physicochemical Properties of Gellan Gum Samples

		HAGG	LAGG
acyl content[a] (%)	glycerate	10.0	5.6
	acetate	3.0	2.5
	total	13.0	8.1
counterion composition (μmol/g)[b]	Na	560.2 ± 29.3	563.3 ± 51.3
	K	ND[c]	ND[c]
	Ca	5.5 ± 1.1	6.9 ± 1.1

[a] Data from the manufacturer by high-performance ion chromatography. [b] Means ± SD of triplicate measurements by inductively coupled plasma optical emission spectrometry. [c] Not detected.

Aqueous Solutions of Gellan Gum. Aqueous solutions of gellan gum were prepared at concentrations sufficient to form molecular assemblies, including associations, gels, and gel precursors. For rheological measurements, each gellan gum sample was dissolved in deionized water at 20 mg/mL with mechanical stirring at 90 °C for 10 min. Aqueous solutions of NaCl or KCl were prepared separately at 0.2 M without heating, whereas those of $CaCl_2$ were prepared at 10 mM also without heating. The gum solutions were mixed with an equivalent volume of each salt solution at 90 °C, resulting in a final concentration of gellan gum of 10 mg/mL and final concentrations of salts of 0.1 M for NaCl or KCl and of 5 mM for $CaCl_2$. Control treatment was prepared in the same manner using deionized water instead of the salt solutions. For the AFM imaging, each gellan gum sample was hydrated in deionized water at 200 μg/mL with gentle stirring at room temperature and then dissolved by heating at 90 °C for 1 h with an occasional vortex mixing every 10 min. Aqueous solutions of NaCl or KCl were prepared separately at 2 mM without heating, whereas those of $CaCl_2$ were prepared at 0.1 mM also without heating. The gum solutions were mixed with an equivalent volume of each salt solution at 90 °C, resulting in a final concentration of gellan gum of 100 μg/mL and final concentrations of salts of 1 mM for NaCl or KCl and of 0.05 mM for $CaCl_2$. After being cooled to room temperature, the mixture was diluted further with deionized water at 20 °C to 1 μg/mL gellan gum and to 0.01 mM or 0.5 μM salts. Control treatment was prepared in the same manner using deionized water instead of the salt solutions.

Rheological Measurements. Consecutive thermal scanning rheological measurements were carried out using an ARES strain-controlled rheometer (Rheometric Scientific, Piscataway, NJ) equipped with a temperature-controlled water bath to determine the temperature dependence of the dynamic storage modulus (G') and dynamic mechanical loss tangent (tan δ) defined by G''/G' (G'' = dynamic loss modulus). Aqueous solutions of gellan gum (10 mg/mL) were placed into a double-wall Couette (bob and cup) geometry (cup inner diameter 34 mm, bob outer diameter 32 mm, gap 1 mm) as hot solutions at 90 °C after adjustment of the weight using deionized water. The geometry was preheated above 90 °C to avoid gelation in sample loading. Soon after that, the surface of the sample was covered by a thin layer of silicone oil to avoid water evaporation during measurement. After being held at 90 °C for 10 min, the temperature decreased from 90 to 20 °C at a constant rate of 0.2 °C/min and then increased from 20 to 90 °C at the same rate. The applied strain was controlled automatically within the linear viscoelastic region throughout the measurements, and the frequency was fixed at 6.28 rad/s (i.e., 1 Hz). The gelling temperature was determined as the intersection of the steepest slope for the portion of the rapid increase in G' and the horizontal axis (*27, 28, 32*). Thermal

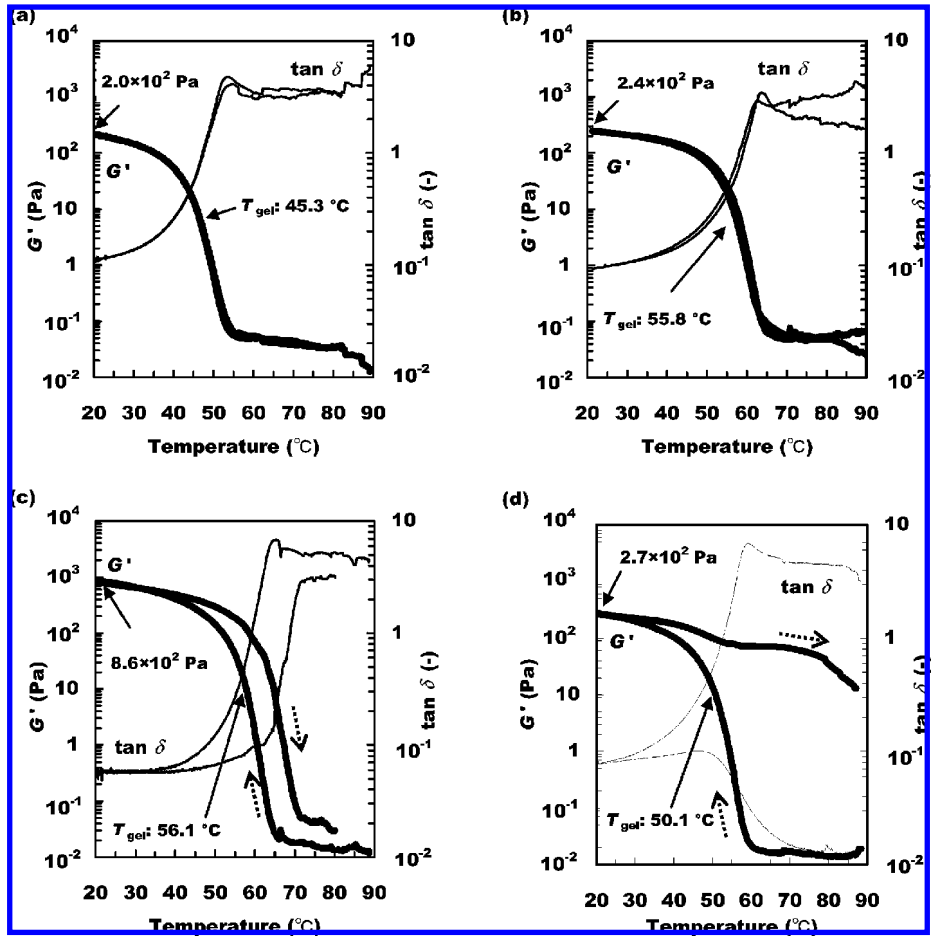

Figure 1. Temperature dependence of G' and tan δ for aqueous solutions of the HAGG sample in the presence or absence of added salts: (**a**) no added salts; (**b**) 0.1 M NaCl; (**c**) 0.1 M KCl; (**d**) 5 mM $CaCl_2$. The concentration of gellan gum was 10 mg/mL in the test solutions. T_{gel} represents the gelling temperature.

hysteresis was identified as the deviation between the descending curves (sol-to-gel transition) and the ascending curves (gel-to-sol transition). Dynamic frequency-sweep measurements were carried out from 10^{-1} to 10^{2} rad/s at a constant temperature of 20 °C (at an intermediate stage during consecutive thermal scanning rheological measurements) and at a fixed strain of 0.1% to determine the relationships between the dynamic complex viscosity (η^*) and frequency (ω):

$$\eta^* = K\omega^{-n} \quad (0 < n < 1) \tag{1}$$

where η^* is defined by $\{(G'^2 + G'^2)^{1/2}\}/i\omega$. The constant K represents the dynamic consistency index and the exponent n the dynamic power-law factor. When n is equal to 1, the system is completely elastic, and η^* decreases with increasing ω. When n is equal to 0, on the other hand, the system is completely viscous, and η^* stays constant regardless of ω (*33*). Each type of measurement was repeated twice to confirm the reproducibility.

AFM Imaging. A multimode scanning probe microscope (Digital Instrument, Inc., Santa Barbara, CA) equipped with a J scanner and a Nanoscope 3 controller was used to image the molecular structures or assemblies for each gellan gum sample. Imaging was carried out in air at ambient temperature and humidity using freshly cleaved mica as the surface. The tapping mode was employed at a drive frequency of ca. 300 kHz using a beam-shaped silicon cantilever of 125 μm nominal length and of 40 N/m nominal spring constant. Aliquots (2 μL) of each gellan gum sample (1 μg/mL) in an aqueous solution were deposited onto a freshly cleaved mica surface and then dried at ambient temperature and humidity for 15 min prior to imaging. Topographical images scanned at 2 Hz and stored in 128 × 128 pixel format were processed using Nanoscope version 5.12r5 software (Digital Instrument, Inc.) to estimate the vertical height and the horizontal width of the molecular features. Data on the vertical height are presented as means ± SD of 30 individual measurements, and the variation in height is presented by the coefficient of variation (CV; %). The horizontal widths were measured at the half-height position of the molecular features, the data of which not being very quantitative as they were due to the curvature radius of the AFM tip, affecting the contact between the tip and the sample and resulting in overestimations in most cases. Therefore, the "measured widths" were calibrated using the following equations to estimate "real widths" by eliminating the tip broadening effect under an assumption that each molecular feature visualized is in a cylindrical shape (*34*):

$$r = w_m^2/16R \quad w_r = 2r \tag{2}$$

where r and R represent the radii of the cylindrical feature and the AFM tip (i.e., 10 nm), respectively. Also, w_m and w_r stand for the widths before and after calibration, respectively. The data calibrated are presented as means ± SD of at least 10 individual measurements, and the variation is also presented by the CV (%).

Statistics. Data on the vertical height from the AFM experiments were examined by analysis of variance with the significance defined at $p < 0.05$. Significant differences among mean values were determined by the Bonferroni test at the same significance level.

RESULTS AND DISCUSSION

Characterizations of Gellan Gum Samples. HAGG (13.0%) was higher in acyl content, represented by the sum of glycerate and acetate, than LAGG (8.1%) (**Table 1**). Glycerate was more sensitive to alkaline deacylation than acetate. Counterions were converted almost completely to sodium for each gellan gum sample. The M_w values were comparable between the two samples, 1.9×10^5 and 1.8×10^5 g/mol for HAGG and LAGG,

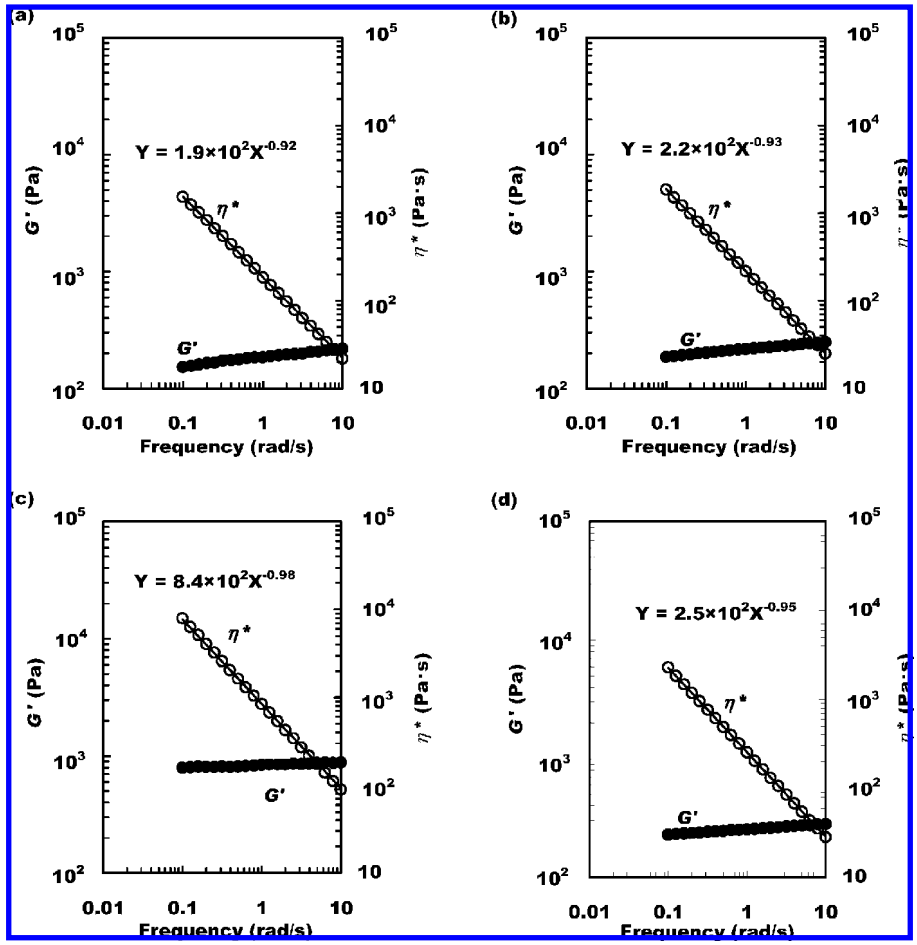

Figure 2. Frequency dependence of G' and η^* for aqueous solutions of the HAGG sample in the presence or absence of added salts at 20 °C: (**a**) no added salts; (**b**) 0.1 M NaCl; (**c**) 0.1 M KCl; (**d**) 5 mM $CaCl_2$. The concentration of gellan gum was 10 mg/mL in the test solutions. *X* and *Y* in the inset regressions represent the frequency and η^*, respectively.

respectively. Since the M_w was determined using a cadoxen as a solvent to prevent unfavorable molecular associations, the data obtained correspond to those of the monomer. Cadoxen is known as a good solvent for cellulose (*35*) and xanthan gum (*36, 37*). As a monomer equivalent, the M_w for LAGG was larger than those reported previously using deacylated gellan gum, ca. $9.5-12.0 \times 10^4$ g/mol (*38−41*), which may be attributed to a mild deacylation process in the present study, preventing depolymerization of the backbone during the process. Since there are no marked differences in the M_w or counterion between the samples, the results are mainly associated with salts added and the acyl content.

Rheological Measurements. *High-Acyl Gellan Gum.* The temperature dependence of G' and tan δ showed that HAGG formed gel structures in the presence or absence of added salts on lowering the temperature (**Figure 1**). No thermal hysteresis was observed between the sol-to-gel and gel-to-sol transitions in the absence of added salts and in the presence of NaCl, whereas hysteresis was detected in the presence of KCl or $CaCl_2$, particularly $CaCl_2$. The ascending curve for $CaCl_2$ showed a two-step decrease in G', indicating the formation of gel structures with different thermal stabilities. G' at 20 °C was larger in the order no added salts (2.0×10^2 Pa) < NaCl (2.4×10^2 Pa) < $CaCl_2$ (2.7×10^2 Pa) < KCl (8.6×10^2 Pa). When compared between the monovalent cations, the effect of potassium on G' was ca. 3.5 times greater than that of sodium. These results may be a reflection of increased thermal stability of network structures and increased energy stored there upon the addition of potassium as found for κ-carrageenan (*42*). The gelling temperature was higher in the order no added salts (45.3 °C) < $CaCl_2$ (50.1 °C) < NaCl (55.8 °C) < KCl (56.1 °C). No marked differences were seen in the gelling temperature between the monovalent cations, which agrees with previous results (*32*). This indicates that the effect of cations on the sol-to-gel transition can be attributed predominantly to electrostatic shielding. The frequency dependence of G' and η^* showed that G' was frequency-dependent in the absence of added salts and in the presence of NaCl, while it was almost frequency-independent in the presence of KCl (**Figure 2**). The effect of $CaCl_2$ was intermediate between NaCl and KCl. The exponent *n* was larger in the order no added salts (0.92) < NaCl (0.93) < $CaCl_2$ (0.95) < KCl (0.98), and accordingly, the constant *K* was larger in the order no added salts (1.9×10^2 Pa·s) < NaCl (2.2×10^2 Pa·s) < $CaCl_2$ (2.5×10^2 Pa·s) < KCl (8.4×10^2 Pa·s). These results indicate enhanced elastic character and consistency of the system upon the addition of salts, particularly KCl.

Low-Acyl Gellan Gum. The temperature dependence of G' and tan δ showed that LAGG formed gel structures in the presence or absence of added salts on lowering the temperature (**Figure 3**). No thermal hysteresis was observed between the sol-to-gel and gel-to-sol transitions in the absence of added salts. However, in the presence of salts, hysteresis was detected clearly, the degree of which was larger in the order NaCl < KCl < $CaCl_2$. Hysteresis for LAGG was more apparent than that for HAGG in any case with salts. G' at 20 °C was larger in the order no added salts (8.1×10^1 Pa) < NaCl (1.3×10^3 Pa) < KCl (9.6×10^3 Pa) < $CaCl_2$ (1.9×10^4 Pa). When

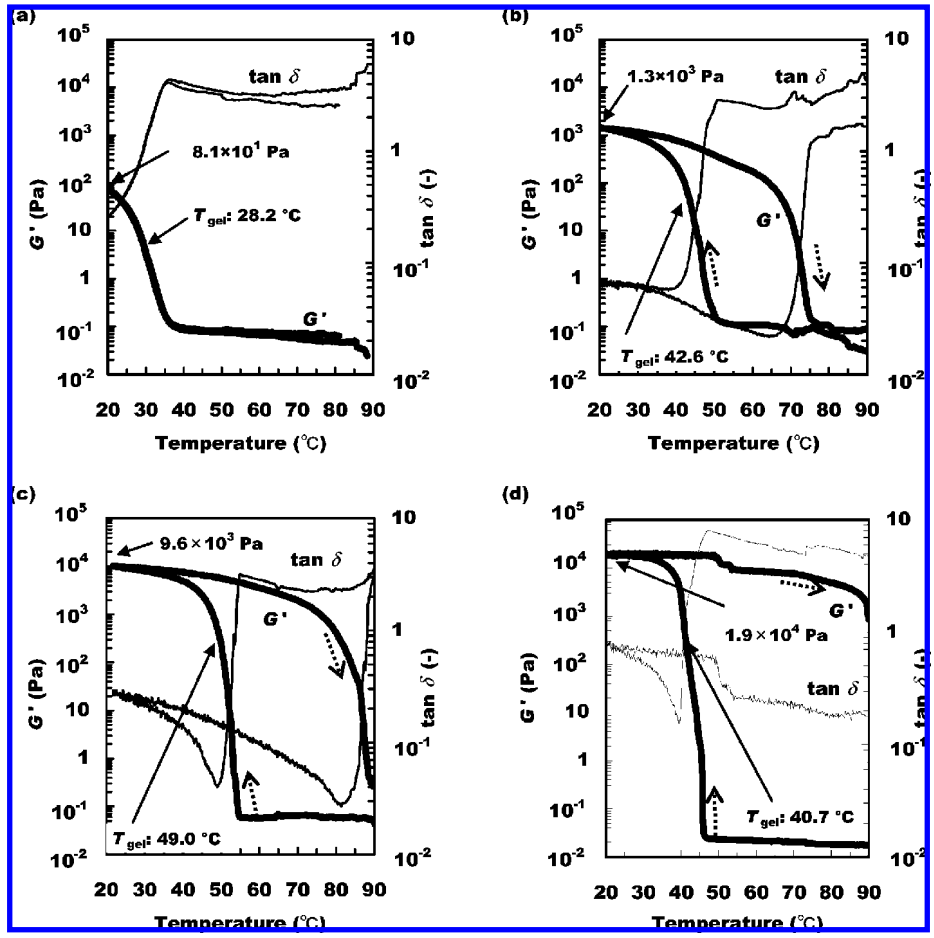

Figure 3. Temperature dependence of G' and tan δ for aqueous solutions of the LAGG sample in the presence or absence of added salts: (**a**) no added salts; (**b**) 0.1 M NaCl; (**c**) 0.1 M KCl; (**d**) 5 mM $CaCl_2$. The concentration of gellan gum was 10 mg/mL in the test solutions. T_{gel} represents the gelling temperature.

compared between the monovalent cations, the effect of potassium on G' was ca. 7 times greater than that of sodium. G' at 20 °C for LAGG was smaller than the corresponding data for HAGG in the absence of added salts, while it was larger in the presence of salts, particularly $CaCl_2$. As in the case of HAGG, the ascending curve for $CaCl_2$ showed a two-step decrease in G', indicating again the formation of gel structures with different thermal stabilities. The gelling temperature was higher in the order no added salts (28.2 °C) < $CaCl_2$ (40.7 °C) < NaCl (42.6 °C) < KCl (49.0 °C), showing a similarity to HAGG but a difference from HAGG in that the gelling temperature for KCl was apparently higher than that for NaCl as reported previously (*28*). These measured gelling temperatures are in accordance with the calculated ones, 45.9 °C for NaCl, 51.0 °C for KCl, and 42.7 °C for $CaCl_2$, using an equation proposed in a previous paper (*28*) for deacylated gellan gum in the presence of cations:

$$T_{gel}^{-1} = A \log(X_p) + B \log(X_i) + C \quad (3)$$

where T_{gel}, X_p, and X_i stand for the gelling temperature (K), polymer concentration (%), and cation concentration (mM), respectively, although there may be a difference in the acyl content in gellan gum between the studies. The gelling temperature for LAGG was lower than that for HAGG in any case, which agrees with previous reports (*32, 43, 44*). The frequency dependence of G' and η^* showed that G' was frequency-dependent in the absence of added salts, while it was almost frequency-independent in the presence of salts (**Figure 4**). The exponent n was larger in the order no added salts (0.78) < NaCl (0.94) < KCl (0.99) < $CaCl_2$ (1.00), and accordingly, the constant K was larger in the order no added salts (3.9×10^1 Pa·s) < NaCl (1.3×10^3 Pa·s) < KCl (1.0×10^4 Pa·s) < $CaCl_2$ (2.6×10^4 Pa·s). These results indicate enhanced elastic character and consistency of the system upon the addition of salts, particularly KCl and $CaCl_2$. These power-law parameters were smaller than those for HAGG in the absence of added salts, and the other way around in the presence of salts with an exception in the presence of NaCl, where n was comparable between the gellan gum samples. Generally, the effects of salts on these rheological characteristics are pronounced more at the lower acyl content.

The results indicate that HAGG forms more elastic gels than LAGG in the absence of added salts but less elastic gels in the presence of salts. In the absence of added salts, acyl groups decrease the charge density within the molecular backbone, which would promote the stabilization of the double helix (particularly via the glycerate group), leading to increased elasticity of the gelled system. Salts reduce electrostatic repulsion between helices, which accounts for the inhibition of interhelical associations and thus the formation of network structures. This effect of salts or cations is pronounced more at the lower acyl content due to reduced steric effects via acyl groups. It has been reported for deacylated gellan gum (*4, 5, 14−19*) that potassium is more effective than sodium in forming mechanically strong gels and increasing thermal stability, and this is also the case for

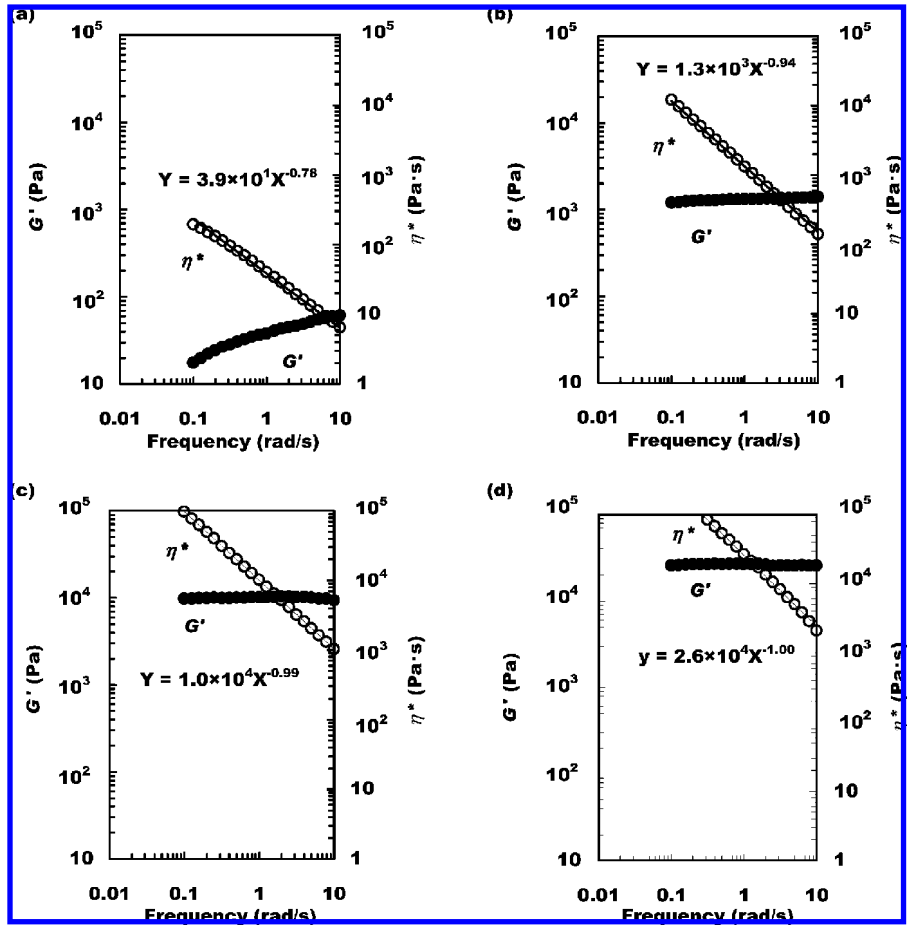

Figure 4. Frequency dependence of G' and η^* for aqueous solutions of the LAGG sample in the presence or absence of added salts at 20 °C: (**a**) no added salts; (**b**) 0.1 M NaCl; (**c**) 0.1 M KCl; (**d**) 5 mM $CaCl_2$. The concentration of gellan gum was 10 mg/mL in the test solutions. *X* and *Y* in the inset regressions represent the frequency and η^*, respectively.

acylated samples. The greater effect of potassium can be attributed to the similarity in size between the hydrodynamic radius of the cation and the cavity which the helix creates, fortifying the structures from both physical and electrostatic aspects.

AFM Imaging. *High-Acyl Gellan Gum.* AFM images showed the differences in molecular assemblies or network structures for HAGG in the presence or absence of added salts (**Figure 5**). For gelling polysaccharides including gellan gum, concentration during air drying may lead to the formation of a flat hydrated film on the substrate in situ which does not exist originally in dilute solutions. Nevertheless, studies on the film are important as a means of testing a model for gelation of polysaccharides in bulk (*45*). Also, it is difficult to understand the macroscopic rheological properties of polysaccharide gels or sols without information about molecular assemblies or network structures because polysaccharides do not function as individual molecules in real systems.

In the absence of added salts and in the presence of NaCl or KCl, none of the images showed continuous network structures but identified branches with observable ends. In the presence of $CaCl_2$, on the contrary, continuous network structures were visible with some inhomogeneities. This structural continuousness relates to enlarged thermal hysteresis in rheological measurements. End-to-end-type interhelical associations do not occur to any great extent on helix formation in the presence of NaCl or KCl, where the branching may arise from the formation of multiple interchain associations because the widths of the fibrils are relatively constant along their length. The fibrils visualized were stretched and elongated in the presence of salts with occasional cyclic features, which may form as a result of intramolecular associations rather than intermolecular ones, similar to the behaviors of ι-carrageenan (*46*) and scleroglucan (*47*). The average vertical height of the fibrils on the image was 0.95 nm in the absence of added salts, which did not change significantly upon the addition of salts. The height of the fibrils was larger than that of a double helix of gellan gum (ca. 0.5 nm) determined by small-angle X-ray scattering using a deacylated sample (*17*), indicating that side-by-side-type interhelical associations do occur locally in any case. The electrostatic effect of salts in minimizing repulsion is distinguishable among cationic species on end-to-end-type interhelical associations, leading to the differences in the formation of network structures. This effect of $CaCl_2$ (0.5 μM) is at least 10 times as great as that of NaCl or KCl (0.01 mM) when compared on the charge equivalent. The steric effect of acyl groups in inhibiting interhelical associations is pronounced on side-by-side-type ones, which may eliminate the differences in the effect among salts, resulting in no apparent differences in the vertical height on the images. Variation in the vertical height of the fibrils (CV) was 17.1% in the absence of added salts. It increased to 20.4% and 24.1% upon the addition of NaCl and $CaCl_2$, respectively, while it decreased to 14.3% upon the addition of KCl. The height exhibited the sharpest distribution pattern in the presence of KCl, but showed a broader pattern in the presence of NaCl

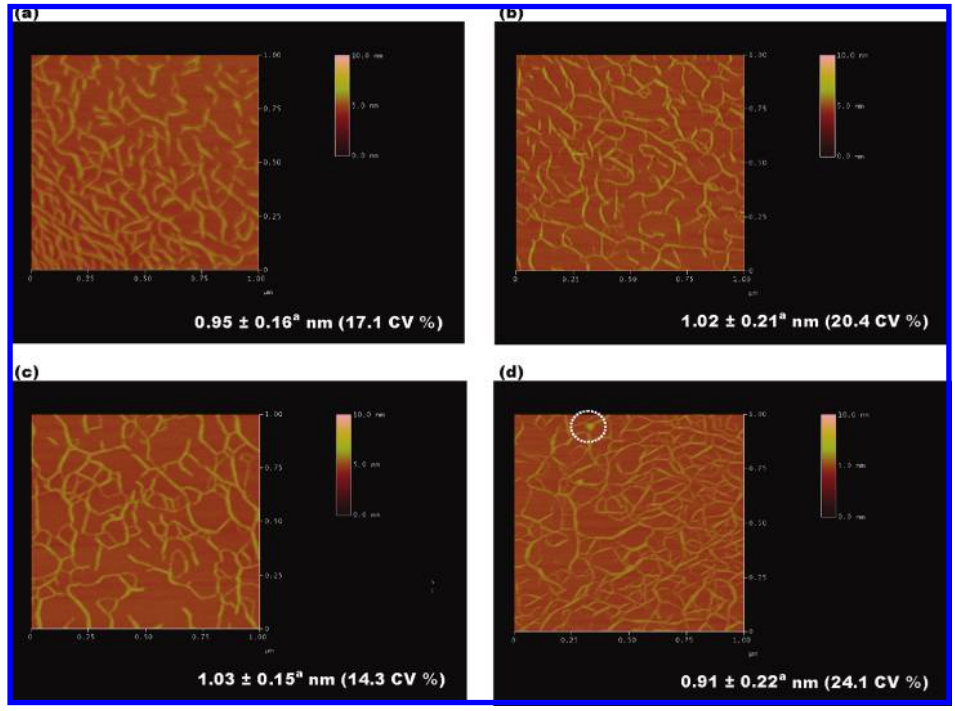

Figure 5. Topographical AFM images of the HAGG sample in the presence or absence of added salts in air: (**a**) no added salts; (**b**) 0.01 mM NaCl; (**c**) 0.01 mM KCl; (**d**) 0.5 μM $CaCl_2$. The concentration of gellan gum was 1 μg/mL in the test solutions. The scanning size of all images is 1 μm × 1 μm. The inset data are on vertical height presented as means ± SD of 30 individual measurements with their CV (%) in parentheses. Data with different superscripts are significantly different at $p < 0.05$.

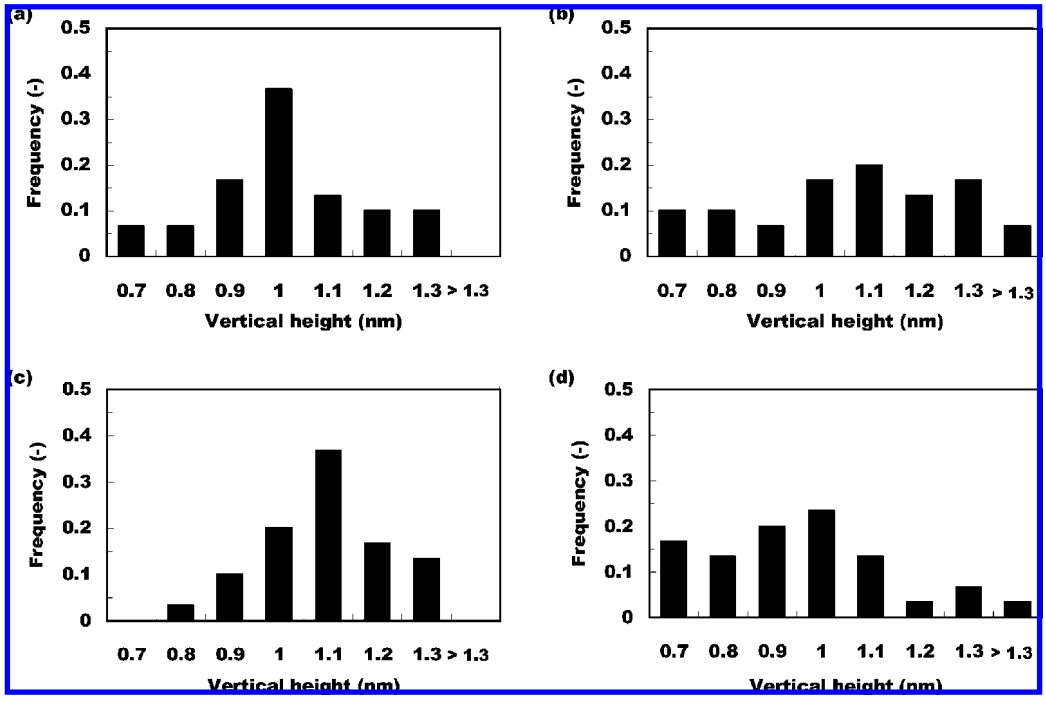

Figure 6. Distribution (histogram) of the vertical height in AFM images for the HAGG sample in the presence or absence of added salts: (**a**) no added salts; (**b**) 0.01 mM NaCl; (**c**) 0.01 mM KCl; (**d**) 0.5 μM $CaCl_2$. The data were from 30 individual measurements using the images in **Figure 5**.

or $CaCl_2$ than in the absence of added salts (**Figure 6**). Particularly, in the presence of $CaCl_2$, a marked increase in height was found sporadically at cross sections between the fibrils as circled in image **d**, contributing to an increased CV (%). Molecular assemblies exhibited a more heterogeneous population of fibrils with various heights in the presence of NaCl or $CaCl_2$. However, in the presence of KCl, the assemblies were more homogeneous, contributing to an increase of the elasticity of the system as represented by an increased G' in rheological measurements. This may be attributed to the fact that potassium ions bind continuously with the helices along the length of the fibrils, leading to the uniformity of the molecular assemblies. The average horizontal width of the fibrils and its variation (CV) were 8.52 nm and 19.3% in the absence of added salts.

The results support the fibrous model (*11*−*14*) as the gelation mechanism of gellan gum, whereby nonassociated fibrils give rise to elasticity via either elongation or branching. The elasticity

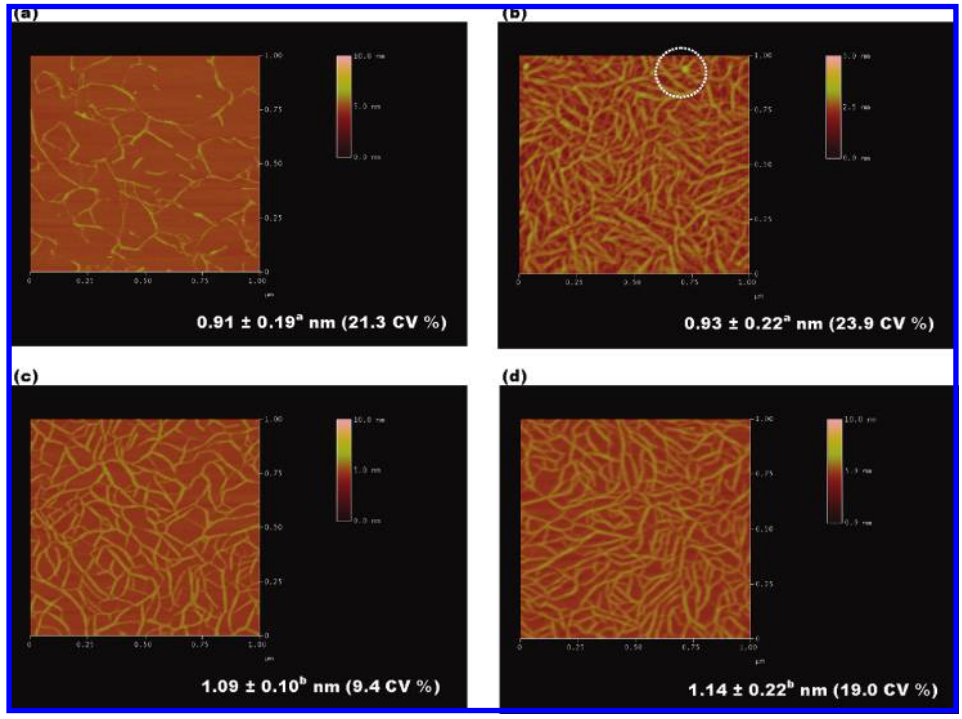

Figure 7. Topographical AFM images of the LAGG sample in the presence or absence of added salts in air: (**a**) no added salts; (**b**) 0.01 mM NaCl; (**c**) 0.01 mM KCl; (**d**) 0.5 μM $CaCl_2$. The concentration of gellan gum was 1 μg/mL in the test solutions. The scanning size of all images is 1 μm $\times$ 1 μm. The inset data are on vertical height presented as means $\pm$ SD of 30 individual measurements with their CV (%) in parentheses. Data with different superscripts are significantly different at $p < 0.05$.

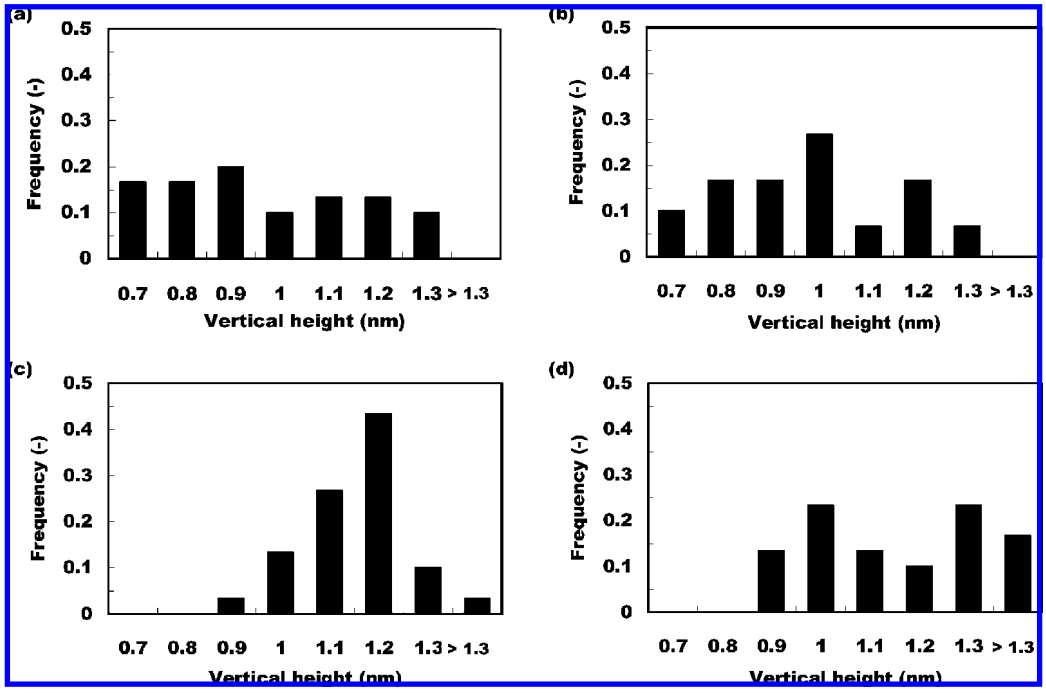

Figure 8. Distribution (histogram) of the vertical height in AFM images for the LAGG sample in the presence or absence of added salts: (**a**) no added salts; (**b**) 0.01 mM NaCl; (**c**) 0.01 mM KCl; (**d**) 0.5 μM $CaCl_2$. The data were from 30 individual measurements using the images in **Figure 7**.

arises mainly from energetic stretching and bending of the fibrils rather than from entropic rubber-like contributions of flexible polymer chains linking adjacent junction zones though the contribution of entropy elasticity is not completely negligible as reported for composite gel systems containing two types of gellan gum with different acyl contents as a matrix and calcium as a cross-linker (*48*).

Low-Acyl Gellan Gum. AFM images showed the differences in molecular assemblies or network structures for LAGG in the presence or absence of added salts (**Figure 7**). In the absence of added salts, no continuous network structures were visualized as in the case of HAGG, which is consistent with the rheological data, showing no thermal hysteresis. The fibrils were more stretched and dispersed than those of HAGG, which can be attributed to increased charge density within the backbone due to the decrease in acyl content. The average vertical height in the image and its variation (CV) were 0.91 nm and 21.3%, respectively. The height was almost

equivalent to, but its variation was larger than, the corresponding data for HAGG. This indicates that LAGG forms more heterogeneous network structures, relating to decreased elasticity of the system. The average horizontal width and its variation (CV) were 3.57 nm and 16.2%, respectively, both of which were smaller than the corresponding data for HAGG. A decreased width indicates a lower degree of interhelical associations, which may be due to increased charge density.

In the presence of salts, continuous network structures were identified, which is consistent with the rheological data, showing enlarged thermal hysteresis. It seemed that network structures were tightly packed in the presence of NaCl or $CaCl_2$, whereas the structures were extended in the presence of KCl. The effect of salts is greater at the lower acyl content on the formation of end-to-end-type interhelical associations due to reduced steric hindrance via acyl groups. There was no evidence of large aggregated or crystalline domains in accordance with a previous paper (*49*). The average vertical height in the image increased significantly upon the addition of KCl or $CaCl_2$ and was larger in the order NaCl (0.93 nm) < KCl (1.09 nm) < $CaCl_2$ (1.14 nm). In comparison with the corresponding data for HAGG, however, the height did not change significantly upon the addition of NaCl or KCl. These results indicate that side-by-side-type interhelical associations do occur locally but that the associations are not enhanced drastically at the lower acyl content in the presence of monovalent cations. These observations may emphasize a role of end-to-end-type interhelical associations in forming network structures and in determining rheological characteristics of the gelled system. Variation in the vertical height (CV) increased to 23.9% upon the addition of NaCl, involving a sporadic marked increase in height as circled in image **b**. It decreased, in contrast, to 9.4% and 19.0% upon the addition of KCl and $CaCl_2$, respectively, both of which were smaller than the corresponding data for HAGG. The height exhibited the sharpest distribution pattern in the presence of KCl as in the case of HAGG, but showed a bimodal pattern in the presence of NaCl or $CaCl_2$ (**Figure 8**). The fibrils were fairly uniform in height with no preferential alignment in the presence of KCl. Formation of highly homogeneous network structures relates to increased elasticity and consistency of the system in the presence of KCl. Structural inhomogeneity is responsible for the stepwise change in G' of the system in the presence of $CaCl_2$, where molecular assemblies extremely large in size (i.e., >1.3 μm) may contribute to an increase in elasticity to a great extent. It is assumed that side-by-side-type interhelical associations can increase elasticity even in inhomogeneous form if the continuousness of the system is ensured through end-to-end-type interhelical associations.

In conclusion, from the relationship between supermolecular structures and rheological properties during the gelation process of gellan gum in the presence or absence of various cations, the continuousness of the network structures relates to thermal hysteresis of the system as a result of end-to-end-type interhelical associations. Calcium is the most effective on the basis of the function to shield electrostatic repulsion between the helices. The homogeneity of the network structures relates to the elasticity and consistency of the system as a result of side-by-side-type interhelical associations with a considerable length. Potassium is the most effective on the basis of the similarity in size between the hydrodynamic radius of the cation and the cavity which the helix creates. The effects of cations are pronounced more at the lower acyl content due to reduced steric effects via acyl groups in inhibiting interhelical associations.

LITERATURE CITED

(1) Jansson, P. E.; Lindberg, B.; Sandford, P. A. Structural studies of gellan gum, an extracellular polysaccharide elaborated by *Pseudomonas elodea*. *Carbohydr. Res.* **1983**, *124*, 135–139.

(2) O'Neill, M. A.; Selvendran, R. R.; Morris, V. J. Structure of the acidic extracellular gelling polysaccharide produced by *Pseudomonas elodea*. *Carbohydr. Res.* **1983**, *124*, 123–133.

(3) Kuo, M. S.; Mort, A. J.; Dell, A. Identification and location of L-glycerate, an unusual acyl substituent in gellan gum. *Carbohydr. Res.* **1986**, *156*, 173–187.

(4) Morris, V. J. Bacterial polysaccharides. In *Food Polysaccharides and Their Applications*; Stephen, A. M., Ed.; Marcel Dekker: New York, 1995; pp 341−375.

(5) Morris, V. J. Bacterial polysaccharides. In *Food Polysaccharides and Their Applications*, 2nd ed.; Stephen, A. M., Phillips, G. O., Williams, P. A., Eds.; Taylor & Francis Group: London, 2006; pp 413−454.

(6) Nishinari, K. Properties of gellan gum. In *Gums and Stabilisers for the Food Industry*; Phillips, G. O., Williams, P. A., Wedlock, D. J., Eds.; The Royal Society of Chemistry: Cambridge, U.K., 1996; Vol. 6, pp 371−383.

(7) Morris, V. J. Gelation of polysaccharides. In *Functional Properties of Food Macromolecules*, 2nd ed.; Hill, S. E., Ledward, D. A., Mitchell, J. R., Eds.; Aspen Publishers: Gaithersburg, MD, 1998; pp 151−226.

(8) Rinaudo, M.; Milas, M. Gellan gum, a bacterial gelling polymer. In *Novel Macromolecules in Food Systems*; Doxastakis, G., Kiosseoglou, V., Eds.; Elsevier: Amsterdam, 2000; pp 239−263.

(9) Sworn, G. Gellan gum. In *Handbook of Hydrocolloids*; Phillips, G. O., Williams, P. A., Eds.; Woodhead Publishing: Cambridge, U.K., 2000; pp 117−135.

(10) Robinson, G.; Manning, C. E.; Morris, E. R. Conformation and physical properties of the bacterial polysaccharides gellan, welan, and rhamsan. In *Food Polymers, Gels and Colloids*; Dickinson, E., Ed.; The Royal Society of Chemistry: London, 1991; pp 22−33.

(11) Gunning, A. P.; Kirby, A. R.; Ridout, M. J.; Brownsey, G. J.; Morris, V. J. Investigation of gellan networks and gels by atomic force microscopy. *Macromolecules* **1996**, *29*, 6791–6796.

(12) Gunning, A. P.; Morris, V. J. Light scattering studies of tetramethyl ammonium gellan. *Int. J. Biol. Macromol.* **1990**, *12*, 338–341.

(13) Morris, V. J.; Kirby, A. R.; Gunning, A. P. A fibrous model for gellan gels from atomic force microscopy studies. *Prog. Colloid Polym. Sci.* **1999**, *114*, 102–108.

(14) Ikeda, S.; Nitta, Y.; Temsiripong, T.; Pongsawatmanit, R; Nishinari, K. Atomic force microscopy studies on cation-induced network formation of gellan. *Food Hydrocolloids* **2004**, *18*, 727–735.

(15) Sanderson, G. R.; Clark, R. C. Gellan gum: Laboratory-produced microbial polysaccharide has many potential food applications as a gelling, stabilizing, and texturizing agent. *Food Technol.* **1983**, *37*, 63–70.

(16) Miyoshi, E.; Nishinari, K. Rheological and thermal properties near the sol-gel transition of gellan gum aqueous solutions. *Prog. Colloid Polym. Sci.* **1999**, *114*, 68–82.

(17) Yuguchi, Y.; Urakawa, H.; Kitamura, S.; Wataoka, I.; Kajiwara, K. The sol-gel transition of gellan gum aqueous solutions in the presence of various metal salts. *Prog. Colloid Polym. Sci.* **1999**, *114*, 41–47.

(18) Ogawa, E.; Matsuzawa, H.; Iwahashi, M. Conformational transition of gellan gum of sodium, lithium, and potassium types in aqueous solutions. *Food Hydrocolloids* **2002**, *16*, 1–9.

(19) Yuguchi, Y.; Urakawa, H.; Kajiwara, K. The effect of potassium salt on the structural characteristics of gellan gum gel. *Food Hydrocolloids* **2002**, *16*, 191–195.

(20) Chandrasekaran, R.; Thailambal, V. G. The influence of calcium ions, acetate and L-glycerate groups on the gellan double-helix. *Carbohydr. Polym.* **1990**, *12*, 431–442.
(21) Chandrasekaran, R.; Puigjaner, L. C.; Joyce, K. L.; Arnott, S. Cation interactions in gellan: An X-ray study of the potassium salt. *Carbohydr. Res.* **1988**, *181*, 23–40.
(22) Tang, J.; Tung, M. A.; Zeng, Y. Compression strength and deformation of gellan gels formed with mono- and divalent cations. *Carbohydr. Polym.* **1996**, *29*, 11–16.
(23) Shoraku, A.; Takigawa, T.; Masuda, T. Effects of alkaline metal salts on viscosity of gellan aqueous solutions. Nihon Reoroji Gakkaishi. *J. Soc. Rheol., Jpn.* **2002**, *30*, 13–17.
(24) Miyoshi, E.; Takaya, T.; Nishinari, K. Gel-sol transition in gellan gum solutions. I. Rheological studies on the effects of salts. *Food Hydrocolloids* **1994**, *8*, 505–527.
(25) Miyoshi, E.; Takaya, T.; Nishinari, K. Gel-sol transition in gellan gum solutions. II. DSC studies on the effects of salts. *Food Hydrocolloids* **1994**, *8*, 529–542.
(26) Matsukawa, S.; Huang, Z.; Watanabe, T. Structural change of polymer chains of gellan monitored by circular dichroism. *Prog. Colloid Polym. Sci.* **1999**, *114*, 92–97.
(27) Tang, J.; Tung, M. A.; Zeng, Y. Gelling temperature of gellan solutions containing calcium ions. *J. Food Sci.* **1997**, *62*, 276–280.
(28) Tang, J.; Tung, M. A.; Zeng, Y. Gelling properties of gellan solutions containing monovalent and divalent cations. *J. Food Sci.* **1997**, *62*, 688−692, 712.
(29) Nitta, Y.; Ikeda, S.; Nishinari, K. The reinforcement of gellan gel network by the immersion into salt solution. *Int. J. Biol. Macromol.* **2006**, *38*, 145–147.
(30) Funami, T.; Hiroe, M.; Noda, S.; Asai, I.; Ikeda, S.; Nishinari, K. Influence of molecular structure imaged with atomic force microscopy on the rheological behavior of carrageenan aqueous system in the presence or absence of cations. *Food Hydrocolloids* **2007**, *21*, 617–629.
(31) Huang, L.; Takahashi, R.; Kobayashi, S.; Kawase, T.; Nishinari, K. Gelation behavior of native and acetylated konjac glucomannan. *Biomacromolecules* **2002**, *3*, 1296–1303.
(32) Huang, Y.; Singh, P. P.; Tang, J.; Swanson, B. G. Gelling temperatures of high acyl gellan as affected by monovalent and divalent cations with dynamic rheological analysis. *Carbohydr. Polym.* **2004**, *56*, 27–33.
(33) Keogh, M. K.; O'Kennedy, B. T. Rheology of stirred yogurt as affected by added milk fat, protein and hydrocolloids. *J. Food Sci.* **1998**, *63*, 108–112.
(34) Morris, V. J.; Gunning, A. P.; Kirby, A. R.; Round, A.; Waldron, K.; Ng, A. Atomic force microscopy of plant cell walls, plant cell wall polysaccharides and gels. *Int. J. Biol. Macromol.* **1997**, *21*, 61–66.
(35) Bao, Y. T.; Bose, A.; Ladisch, M. R.; Tsao, G. T. New approach to aqueous gel permeation chromatography of nonderivatized cellulose. *J. Appl. Polym. Sci.* **1980**, *25*, 263–275.
(36) Sato, T.; Norisuye, T.; Fujita, H. Double-stranded helix of xanthan in dilute solution: evidence from light scattering. *Polym. J.* **1984**, *16*, 341–350.
(37) Milas, M.; Tinland, B. Behaviour of xanthan in cadoxen. *Carbohydr. Polym.* **1990**, *13*, 47–56.
(38) Okamoto, T.; Kubota, K.; Kuwahara, N. Light scattering study of gellan gum. *Food Hydrocolloids* **1993**, *7*, 363–371.
(39) Takahashi, R.; Akutu, M.; Kubota, K.; Nakamura, K. Characterization of gellan gum in aqueous NaCl solution. *Prog. Colloid Polym. Sci.* **1999**, *114*, 1–7.
(40) Takahashi, R.; Tokunou, H.; Kubota, K.; Ogawa, E.; Oida, T.; Kawase, T.; Nishinari, K. Solution properties of gellan gum: change in chain stiffness between single- and double- stranded chains. *Biomacromolecules* **2004**, *5*, 516–523.
(41) Ogawa, E.; Takahashi, R.; Yajima, H.; Nishinari, K. Effects of molar mass on the coil to helix transition of sodium-type gellan gums in aqueous solutions. *Food Hydrocolloids* **2006**, *20*, 378–385.
(42) Piculell, L. Gelling carrageenans. In *Food Polysaccharides and Their Applications*; Stephen, A. M., Ed.; Marcel Dekker: New York, 1995; pp 205−244.
(43) Mao, R.; Tang, J.; Swanson, B. G. Texture properties of high and low acyl mixed gellan gels. *Carbohydr. Polym.* **2000**, *41*, 331–338.
(44) Matsukawa, S.; Watanabe, T. Gelation mechanism and network structure of mixed solution of low- and high-acyl gellan studied by dynamic viscoelasticity, CD and NMR measurements. *Food Hydrocolloids* **2007**, *21*, 1355–1361.
(45) Morris, V. J. Applications of atomic force microscopy in food science. In *Gums and Stabilisers for the Food Industry*; Williams, P. A., Phillips, G. O., Eds.; The Royal Society of Chemistry: Cambridge, U.K., 1998; Vol. 9, pp 361−370.
(46) McIntire, T. M.; Brant, D. A. Imaging of carrageenan macrocycles and amylose using noncontact atomic force microscopy. *Int. J. Biol. Macromol.* **1999**, *26*, 303–310.
(47) Morris, V. J.; Kirby, A. R.; Gunning, A. P. Macromolecules—polysaccharides. In *Atomic Force Microscopy for Biologists*; Morris, V. J., Kirby, A. R., Gunning, A. P., Eds.; Imperial College Press: London, 1999; pp 105−123.
(48) Mao, R.; Tang, J.; Swanson, B. G. Texture properties of gellan gels as affected by temperature. *J. Texture Stud.* **1999**, *30*, 409–433.
(49) Kirby, A. R.; Gunning, A. P.; Morris, V. J. Imaging polysaccharides by atomic force microscopy. *Biopolymers* **1996**, *38*, 355–366.

Received for review March 12, 2008. Revised manuscript received June 19, 2008. Accepted June 20, 2008.

JF8007713